Intramolecular Bridge/Terminal Oxo Exchange within $[Mo^{V}_2O_3]^{4+}$ Complexes Containing Linear Oxo Bridges

Robert L. Thompson, Samkeun Lee, Steven J. Geib, and N. John Cooper*

Department of Chemistry, University of Pittsburgh, Pittsburgh, Pennsylvania 15260

Received June 25, 1993®

Room-temperature ^{13}C NMR spectra of the d^1–d^1 dimer $[Mo_2O_3\{S_2{}^{13}CN(CH_2Ph)_2\}_4]$ (**1**) exhibit a broad singlet for the thiocarboxylate ligand. The molecule is fluxional, and in the low-temperature limit this singlet is replaced by two assymetrical doublets (with components at δ 207.4, 207.2 and δ 200.7, 199.7) assigned to the thiocarboxylate ligands with one S trans to the bridging oxo group and one S trans to the terminal oxo group respectively of the syn and the anti isomers of **1**. The barrier to exchange has been determined between 320 and 335 K from the width of the resonance in the fast exchange region, and the small entropic contribution to the barrier ($\Delta H^{\ddagger} = 11.9 \pm 0.4$ kcal mol^{-1}, $\Delta S^{\ddagger} = -2.0 \pm 0.6$ cal K^{-1} mol^{-1}) argues in favor of an intramolecular mechanism for the exchange reaction in which the thiocarbamate ligands are rendered equivalent by exchange of bridge and terminal oxo groups through a transition state in which the linear oxo bridge has been replaced by two bent oxo bridges. This interpretation is supported by the observation that the related xanthate complexes $[Mo_2O_3(S_2{}^{13}COEt)_4]$ (**4**) and $[Mo_2O_3(S_2{}^{13}CO^{i}Pr)_4]$ (**5**) participate in similar exchange processes with $\Delta H^{\ddagger} = 11.1 \pm 0.3$ and 12.9 ± 0.4 kcal mol^{-1} and $\Delta S^{\ddagger} = -3.9 \pm 1.2$ and 1.9 ± 0.6 cal K^{-1} mol^{-1}, respectively. The small entropic contributions are again consistent with an intramolecular mechanism, and the similarity in enthalpic parameters for **1**, **4**, and **5** argues against a mechanism involving dissociation of the $[Mo^{V}_2O_3]^{4+}$ dimers into $[Mo^{VI}O_2]^{2+}$ and $[Mo^{IV}O]^{2+}$ containing monomers since such disproportionations are ligand sensitive. Single crystal diffraction studies have established that **1** (monoclinic space group $P2_1/n$, with $a = 11.604(4)$ Å, $b = 21.81(2)$ Å, $c = 13.85(1)$ Å, $\beta = 99.90(2)°$, $Z = 2$, and $R = 4.37\%$) and **5** (monoclinic space group $C2/c$, with $a = 25.508(5)$ Å, $b = 9.659(2)$ Å, $c = 14.986(4)$ Å, $\beta = 101.96(2)°$, $Z = 4$, and $R = 5.52\%$) have anti and syn orientations respectively for the terminal oxo groups in the solid state. All three complexes exist as a mixture of syn and anti isomers in solution, establishing that there is only a small free energy difference between these geometries.

Introduction

Oxo complexes play a central role in the biological and inorganic chemistry of molybdenum.[1,2] In the +5 oxidation state molybdenum oxo chemistry is dominated by the $[Mo^{V}_2O_3]^{4+}$ unit, which contains a linear oxo bridge that spin pairs two d^1 centers while two terminal oxo ligands adopt syn or anti orientations perpendicular to the oxo bridge.[2-8]

Our interest in $[Mo^{V}_2O_3]^{4+}$ complexes, stimulated by the unusual photochromism we have observed for some examples[9] and by the potential utilty of such properties in optical memory systems and other optoelectronic applications,[10] recently led us to examine the solution structures of $[Mo^{V}_2O_3]^{4+}$ complexes by ^{13}C NMR. We now wish to report that $[Mo^{V}_2O_3]^{4+}$ complexes with both dithiocarbamate and xanthate ligands exhibit low-energy intramolecular dynamic behavior, which we propose involves bridge for terminal oxo exchange, and that there is only a small free energy difference between the syn and anti isomers in the complexes examined.

Experimental Section

General Procedures. All manipulations were carried out under a dry, oxygen-free nitrogen atmosphere by means of a Vacuum Atmospheres drybox or standard Schlenk techniques. Toluene and hexane were distilled from potassium metal, and methylene chloride was distilled from CaH_2 before use. Pentane was stirred over 5% HNO_3/H_2SO_4, then neutralized with K_2CO_3, and distilled from CaH_2 before use. Deuterated methylene chloride (99.9% D, MSD Isotopes) and chloroform (99.8% D, MSD Isotopes) were degassed by dry nitrogen purge and passed through basic activity I alumina to remove HCl before use. Labeled potassium dibenzyldithiocarbamate was prepared from $^{13}CS_2$ (99.9% ^{13}C, MSD Isotopes) and $HN(CH_2Ph)_2$ according to an adaptation of the procedure described by Colton and Scollary,[11] and unlabelled potassium diben-

* Abstract published in *Advance ACS Abstracts*, September 15, 1993.

(1) (a) Bray, R. C. In *The Enzymes*, 3rd ed.; Boyer, P. D., Ed.; Academic Press: New York, 1975; Vol. XII, Part B, Chapter 6. (b) Stiefel, E. I. *Prog. Inorg. Chem.* **1977**, *22*, 1. (c) Coughlan, M. P., Ed.; *Molybdenum and Molybdenum Containing Enzymes*; Pergamon Press: New York, 1980. (d) Newton, W. E.; Otsuka, S., *Molybdenum Chemistry of Biological Significance*; Plenum Press: New York, 1980. (e) Garner, C. D.; Charnock, J. M. In *Comprehensive Coordination Chemistry* Wilkinson, G., Gillard, R. D., McCleverty, J. A., Eds.; Pergamon: Oxford, England, 1987; Vol. 3, Part 36.4. (f) Holm, R. H. *Coord. Chem. Rev.* **1990**, *100*, 183.

(2) Craig, J. A.; Harlan, E. W.; Snyder, B. S.; Whitener, M. A.; Holm, R. H. *Inorg. Chem.* **1989**, *28*, 2082.

(3) Holm, R. H. *Chem. Rev.* **1987**, *87*, 1401.

(4) Blake, A. B.; Cotton, F. A.; Wood, J. S. *J. Am. Chem. Soc.* **1964**, *86*, 3024.

(5) (a) Knox, J. R.; Prout, C. K. *Acta Crystallogr. B* **1969**, *B25*, 2281. (b) Aliev, Z. G.; Atovmyan, L. O.; Tkachev, V. V. *Zh. Strukt. Khim.* **1975**, *16*, 694. (c) Thompson, R. L.; Geib, S. J.; Cooper, N. J. *Inorg. Chem.*, following paper in this issue.

(6) Bino, A.; Cohen, S.; Tsimering, L. *Inorg. Chim. Acta* **1983**, *77*, L79.

(7) (a) Ricard, L.; Estienne, J.; Karsgiannidis, P.; Toledano, P.; Fischer, J.; Mitschler, A.; Weiss, R. *J. Coord. Chem.* **1974**, *3*, 227. (b) Garner, C. D.; Howlader, N. C.; Mabbs, F. E.; McPhail, A. T.; Onan, K. D. *J. Chem. Soc., Dalton Trans.* **1979**, 962.

(8) Zubieta, J. A.; Maniloff, G. B. *J. Inorg. Nucl. Chem.* **1976**, *12*, 121. (b) Cotton, F. A.; Fanwick, P. E.; Fitch, J. W., III. *Inorg. Chem.* **1978**, *17*, 3254. (c) Tsao, Y. Y.-P.; Fritchie, C. J., Jr.; Levy, H. A. *J. Am. Chem. Soc.* **1978**, *100*, 4089. (d) Tatsumisago, M.; Matsubayashi, G.; Tanaka, T.; Nishigaki, S.; Nakatsu, K. *J. Chem. Soc., Dalton Trans.* **1982**, 121. (e) Dahlstron, P. L.; Hyde, J. R.; Vella, P. A.; Zubieta, J. *Inorg. Chem.* **1982**, *21*, 927. (f) Kamenar, B.; Penavic, M.; Korpar-Colig, B.; Markovic, B. *Inorg. Chem. Acta* **1982**, *65*, L245. (g) Lincoln, S.; Koch, S. A. *Inorg. Chem.* **1986**, *25*, 1594. (h) Baird, D. M.; Rheingold, A. L.; Croll, S. D.; DiCeuso, A. T. *Inorg. Chem.* **1986**, *25*, 3458. (i) El-Essawi, M. M.; Weller, F.; Stahl, K.; Kersting, M.; Dehnicke, K. *Z. Anorg. Allg. Chem.* **1986**, *542*, 175. (j) Mattes, R.; Scholard, H.; Mikloweit, U.; Schrenk, V. *Z. Naturforsch.* **1987**, *42B*, 599.

(9) Lee, S. K.; Staley, D. L.; Rheingold, A. L.; Cooper, N. J. *Inorg. Chem.* **1990**, *29*, 4391.

(10) (a) *Photochromism-Molecules and Systems*; Dürr, H., Bouos-Laurent, H., Eds.; Elsevier: Amsterdam, 1990 (b) Emmelius, M.; Pawlowski, G.; Vollman, H. W. *Angew. Chem., Int. Ed. Engl.* **1989**, *28*, 1445.

(11) Colton, R.; Scollary, G. R. *Aust. J. Chem.* **1968**, *21*, 1427.

0020-1669/93/1332-6067$04.00/0

zyldithiodicarbamate was prepared similarly from CS_2.[11] Labeled potassium isopropyl xanthate and potassium ethyl xanthate were prepared from $^{13}CS_2$ and ^{i}PrOH or EtOH according to an adaptation of the procedure described by Newton et al.[12] Microanalyses were performed by Atlantic Microlabs, Inc., Norcross, GA.

Preparation of $[Mo_2O_3\{S_2{}^{13}CN(CH_2Ph)_2\}_4]\cdot CH_2Cl_2$ ($1\cdot CH_2Cl_2$). Labeled $K[S_2{}^{13}CN(CH_2Ph)_2]$ was used to prepare $[Mo_2O_3\{S_2{}^{13}CN(CH_2Ph)_2\}_4]$ from $MoCl_5$ in H_2O according to the procedure used by Newton et al. for related complexes.[13] Samples of $[Mo_2O_3\{S_2{}^{13}CN(CH_2Ph)_2\}_4]$ were purified by recrystallization from a 3:1 mixture of pentane and CH_2Cl_2 at −30 °C. ^1H NMR (CD_2Cl_2, 300 MHz): δ 7.36–7.27 (m, 40 H, 8 C_6H_5), 4.97 (br m, 16 H, 8 CH_2). $^{13}C\{^1H\}$ NMR ($CDCl_3$, 125 MHz): δ 203.8 (br s, CS_2), 134.4 (s, C_6H_5), 129.0 (s, C_6H_5), 128.5 (s, C_6H_5), 128.4 (s, C_6H_5), 52.6 (s, CH_2). Anal. Calcd for $C_{60}H_{56}Mo_2N_4O_3S_8\cdot CH_2Cl_2$: C, 51.80; H, 4.03; N, 3.96. Found: C, 52.10; H, 4.17; N, 4.00.

Preparation of $[Mo_2O_3\{S_2CN(CH_2Ph)_2\}_4]\cdot CH_2ClCH_2Cl$ ($1\cdot CH_2ClCH_2Cl$). Samples of unlabeled **1** for X-ray diffraction studies were prepared from $MoCl_5$ in a manner identical to that described above for the ^{13}C-labeled material, and crystals suitable for X-ray diffraction were grown by diffusion of hexane vapor into a saturated solution of **1** in CH_2ClCH_2Cl.

Preparation of $[MoO\{S_2CN(CH_2Ph)_2\}_2]$ (2). This compound was prepared by PPh_2Et reduction of $[MoO_2\{S_2CN(CH_2Ph)_2\}_2]$ in refluxing 1,2-dichloroethane by means of an adaptation of the procedure described by Chen et al. for $[MoO(S_2CNEt_2)_2]$.[14] $^{13}C\{^1H\}$ NMR ($CDCl_3$, 74.5 MHz): δ 223.5 (br s, CS_2), 133.6, 129.2, 128.7, 128.4 (all s, C_6H_5), 52.8 (s, CH_2).

Preparation of $[MoO_2\{S_2CN(CH_2Ph)_2\}_2]$ (3). $K[S_2C(CH_2Ph)_2]$ was used to prepare $[MoO_2\{S_2CN(CH_2Ph)_2\}_2]$ from $Na_2MoO_4\cdot 2H_2O$ according to an adaptation of the procedure described by Moore and Larson.[15] $^{13}C\{^1H\}$ NMR (CD_2Cl_2, 74.5 MHz): δ 199.9 (br s, CS_2), 133.6 (s, C_6H_5), 129.3 (s, C_6H_5), 128.7 (s, C_6H_5), 128.4 (s, C_6H_5), 53.7 (s, CH_2).

Preparation of $[Mo_2O_3(S_2{}^{13}COEt)_4]$ (4). Labeled $K[S_2{}^{13}COEt]$ was used to prepare $[Mo_2O_3(S_2{}^{13}COEt)_4]$ from $Na_2MoO_4\cdot 2H_2O$ according to an adaptation of the literature procedures.[12,15] Samples of $[Mo_2O_3(S_2{}^{13}COEt)_4]$ were purified by recrystallization from a 2:1 mixture of pentane and toluene at −30 °C. ^1H NMR (CD_2Cl_2, 300 MHz): δ 4.65 (br m, 8 H, 4 CH_2), 1.49 (t, J = 7.1 Hz, 12 H, 4 CH_3). $^{13}C\{^1H\}$ NMR (CD_2Cl_2, 74.5 MHz): δ 227.1 (br s, CS_2), 71.4 (s, CH_2), 14.0 (s, CH_3). Anal. Calcd for $C_{12}H_{20}Mo_2O_7S_8$: C, 19.89; H, 2.79. Found: C, 19.91; H, 2.73.

Preparation of $[Mo_2O_3(S_2{}^{13}CO^iPr)_4]\cdot C_6H_5CH_3$ ($5\cdot C_6H_5CH_3$). Labeled $K[S_2{}^{13}CO^iPr]$ was used to prepare $[Mo_2O_3(S_2{}^{13}CO^iPr)_4]$ from $Na_2MoO_4\cdot 2H_2O$ according to an adaptation of the literature procedure.[12,15] Samples of $[Mo_2O_3(S_2{}^{13}CO^iPr)_4]$ were purified by recrystallization from a 2:1 mixture of pentane and toluene at −30 °C as a monotoluene solvate. Diffraction quality crystals of unlabeled $[Mo_2O_3(S_2CO^iPr)_4]\cdot C_6H_5CH_3$ (prepared similarly) were grown by the diffusion of hexane vapor into a saturated toluene solution of the complex within a sealed vessel at room temperature over a period of 10 days. Purple hexagonal prisms of $[Mo_2O_3(S_2CO^iPr)_4]\cdot C_6H_5CH_3$ with a green luster were collected by decantation, washed with pentane, and dried under vacuum. ^1H NMR (CD_2Cl_2, 300 MHz): δ 7.25–7.10 (m, 5 H, $C_6H_5CH_3$), 5.51 (septet, J = 6.2 Hz, 4 H, CH), 2.34 (s, 3 H, $CH_3C_6H_5$), 1.46 (d, J = 6.2 Hz, 24 H, 8 CH_3). $^{13}C\{^1H\}$ NMR ($CDCl_3$, 74.5 MHz): δ 225.7 (br s, CS_2), 79.8 (s, CH), 21.6 (s, CH_3). Anal. Calcd for $C_{23}H_{36}Mo_2O_7S_8$: C, 31.65; H, 4.16. Found: C, 31.22; H, 4.08.

Variable-Temperature NMR Studies. ^1H spectra were recorded on a Bruker AF 300 spectrometer at 300 MHz. ^{13}C NMR spectra were recorded on a Bruker AF300 or 500 spectrometer at 74.5 or 125 MHz respectively. Temperatures within the NMR probe were controlled by a Bruker variable-temperature unit, which was calibrated against boiling and freezing distilled H_2O and is accurate to within 0.2 °C. Samples were allowed to equilibrate thermally at each temperature for 10 min before spectra were recorded. The high temperature range was limited to 325 K in $CDCl_3$, 305 K in CD_2Cl_2, and 335 K in 1,2-dichloroethane by the solvent boiling points. Low-temperature spectra were recorded down to 210 K in CD_2Cl_2 and 225 K in $CDCl_3$, below which further changes became negligible. Exchange barriers were calculated from the line widths of ^{13}C resonances arising from exchanging sites using the appropriate equations as follows.

In the case of exchange processes with equal populations in both sites, as established by integration of the low-temperature spectrum, the line width at the lower limit was assumed to be the line width in the absence of exchange, $w^\circ_{1/2}$, and was used to calculate T_2^{eff}.[16,17]

$$T_2^{eff} = 1/(\pi w^\circ_{1/2})$$

This value was then used to calculate the rate of exchange, k, below coalescence using the slow exchange limit approximation.[16,17]

$$k = \pi w_{1/2} - 1/T_2^{eff}$$

The rate of exchange above coalescence was calculated according to the fast exchange approximation[16,17] using the value of $w^\circ_{1/2}$ obtained above coalescence and the value of $\Delta\nu$ obtained in the low-temperature limit.

$$k = \pi(\Delta\nu)^2/2(w_{1/2} - w^\circ_{1/2})$$

For comparison with the line-width data the rate of exchange at coalescence was also calculated using the frequency difference between the resonances below coalescence, $\Delta\nu$, and assuming equal forward and reverse exchange rates so that[16,17]

$$k = \pi\Delta\nu/2^{1/2} = 2.22\Delta\nu$$

The free energies of activation ($\Delta G^\ddagger$) for the exchange processes at each temperature were calculated from exchange rates by means of the Eyring equation,[18] taking the transmission coefficient $\kappa = 1$ as is usual in dynamic NMR studies.[16] The activation enthalpies and entropies ($\Delta H^\ddagger$ and $\Delta S^\ddagger$) were calculated from the intercept and slope of plots of $\Delta G^\ddagger$ vs temperature, treating the values above and below coalescence as separate data sets. The uncertainties in $\Delta G^\ddagger$ were calculated as outlined in ref 17, *eq* 111.

In the case of exchange processes with unequal populations in exchanging sites (as indicated by unequal peak integrations), the temperatures at which spectra with measurable line widths for the smaller peaks could be recorded were few, and free energies of activation were approximated by means of the method described by Shanan-Atidi and Bar-Eli.[19] These free energies of activation for disappearance of the two different species in the secondary exchanges were estimated as follows:

$$\Delta G^\ddagger_A = 4.57T_c\{10.62 + \log[\Delta\nu/k_A(1 - \Delta P)] + \log(T_c/\Delta\nu)\}$$

$$\Delta G^\ddagger_B = 4.57T_c\{10.62 + \log[\Delta\nu/k_B(1 + \Delta P)] + \log(T_c/\Delta\nu)\}$$

where T_c is the coalescence temperature, k_A and k_B are the rate constants obtained using the slow exchange limit approximation for the signals A and B,[16,17] and ΔP is the population difference calculated from the relative integrated areas of signals A and B. The uncertainties for these $\Delta G^\ddagger$ values are estimated to be ca. 20%.

X-ray Diffraction Studies. Deep purple crystals with a green luster of $C_{60}H_{56}Mo_2N_4O_3S_8\cdot CH_2ClCH_2Cl$ ($1\cdot CH_2ClCH_2Cl$) and $C_{16}H_{28}Mo_2O_7S_8\cdot C_6H_5CH_3$ ($5\cdot C_6H_5CH_3$) were coated in epoxy cement and attached to fine glass fibers. Diffraction data were collected for each crystal as summarized in Table I.

$1\cdot CH_2ClCH_2Cl$ was uniquely assignable to the monoclinic group $P2_1/n$ on the basis of systematic absences. On the basis of systematic absences and of photographic evidence **5** was assignable to the monoclinic space group $C2/c$ or Cc. Centrosystematic $C2/c$ was chosen on the basis of E-values and the succesful solution and refinement of the structure. Unit cell dimensions were derived from the least-squares fit of the angular settings of 25 reflections with $18° \le 2\theta \le 25°$ for both crystals. A profile fitting procedure was applied to all data to improve the precision of the measurement of weak reflections. A semiempirical absorption correlation (XEMP) was applied to the diffraction data. Diffraction data were corrected for extinction effects.

Both structures were studied by means of the direct methods routine TREF which located the Mo atoms. The remaining non-hydrogen atoms were located from subsequent Fourier syntheses and refined isotropically.

(12) Newton, W. E.; Corbin, J. L.; McDonald, J. W. *J. Chem. Soc., Dalton Trans.* **1974**, 1044.
(13) Newton, W. E.; Corbin, J. L.; Bravard, D. C.; Searles, J. E.; McDonald, J. W. *Inorg. Chem.* **1974**, *13*, 1100.
(14) Chen, G. J.-J.; McDonald, J. W.; Newton, W. E. *Inorg. Chem.* **1976**, *15*, 2612.
(15) Moore, F. W.; Larson, M. L. *Inorg. Chem.* **1967**, *6*, 998.
(16) Binsch, G. *Top. Stereochem.* **1968**, *3*, 97.
(17) Binsch, G. In *Dynamic Nuclear Magnetic Resonance Spectroscopy*; Jackman, L. M., Cotton, F. A., Eds.; Academic Press: New York, 1975, Chap. 3.
(18) Glasstone, S.; Laidler, K. J.; Eyring, H. *The Theory of Rate Processes*; McGraw-Hill: New York, 1941; p 195.
(19) Shanan-Atidi, H.; Bar-Eli, K. H. *J. Phys. Chem.* **1970**, *74*, 961.

Table I. Summary of Crystal Data, Data Collection, and Refinement Parameters for $[Mo_2O_3\{S_2CN(CH_2Ph)_2\}_2]\cdot 2CH_2ClCH_2Cl$ (**1**·$2CH_2ClCH_2Cl$) and $[Mo_2O_3(S_2CO^iPr)_4\cdot C_6H_5CH_3]$ (**5**·$C_6H_5CH_3$)

	1	**5**
	Crystal Data	
formula	$C_{62}H_{60}Cl_4N_4O_3S_8Mo_2$	$C_{23}H_{36}O_7S_8Mo_2$
cryst syst	monoclinic	monoclinic
space group	$P2_1/n$	$C2/c$
a, Å	11.604(4)	25.508(5)
b, Å	21.81(2)	9.659(2)
c, Å	13.85(1)	14.986(4)
β, deg	99.90(2)	101.96(2)
V, Å^3	3453(4)	3613(1)
Z	2	4
ρ(calcd), g cm^{-3}	1.469	1.605
	Data Collection	
μ, cm^{-1}	8.1	11.9
temp, °C	24	24
cryst dimens, mm	0.22 × 0.26 × 0.34	0.31 × 0.31 × 0.36
radiation	Mo Kα (λ = 0.710 73 Å), graphite-monochromated	
diffractometer	Siemens R3m/V	
scan speed, deg min^{-1}	variable, 5–20	variable, 4–14
2θ scan range, deg	$4 < 2\theta < 50$	$4 < 2\theta < 48$
scan technique	θ–2θ	ω
data collcd	$\pm h,+k,+l$	$+h,+k,\pm l$
weighting factor, g	0.005	0.005
no. of unique data	6094 (6703 read)	5270 (5672 read)
no. of unique data with $F_o > 6(F_o)$	3654	2818
std rflns	3/197	3/197
	Agreement Factors	
R, %	4.37	5.52
R_w, %	6.77	7.63
GOF	0.82	0.87
max peak, e Å^{-3}	0.54	1.07
data:param	9.5:1	16.1:1
Δ/σ	0.016	0.029

Hydrogen atoms were placed in idealized calculated positions (d(C–H) = 0.96 Å). The final difference Fourier syntheses for both compounds showed only diffuse backgrounds. Inspections of F_o vs F_c values and trends based on sin θ, Miller indices and parity groups failed to reveal any systematic errors in the X-ray data for either crystal. Atomic coordinates are listed in Tables II and V, selected bond lengths in Tables III and VI, and selected bond angles in Tables IV and VII. All computer programs used in the collection, solution and refinement of crystal data are contained in the Siemens program packages SHELXTL PLUS (VMS version 4.2).

Results and Discussion

An early theoretical study of a structurally characterized example suggested that the dihedral angle between the two O_t-MoO_b (O_t = terminal oxo, O_b = bridging oxo) planes in $[Mo^{V}_2O_3]^{4+}$ complexes must be close to 0 or 180° if the single valence electron at each metal center is to be spin paired,[4] and X-ray diffraction studies have indeed established that subsequently characterized examples of these complexes adopt either syn or anti geometries in the solid state.[5-8] The local coordination sphere around the Mo atoms within the $[M_2O_3]^{4+}$ core approximates an octahedron, with the remaining coordination sites most typically filled by the sulfur atoms of a bischelating dithio ligand such as a dithiophosphate, an xanthate, or a dithiocarbamate as shown by the selected examples in Scheme I[4,5,7] (although many examples have demonstrated that $[Mo^{V}_2O_3]^{4+}$ complexes are not limited to such ligand systems,[8] and recent examples can be found, for example, in Schiff base systems[2]).

There is a clear distinction in both the syn and the anti geometries between bischelating ligand molecules which have one sulfur atom trans to the bridging oxo and those which have one sulfur trans to a terminal oxo. We were accordingly suprised to discover, in the course of studies of photodisproportionation of the dithiocarbamate complex $[Mo_2O_3\{S_2CN(CH_2Ph)_2\}_4]$ (**1**),[9] that ^{1}H NMR spectra of **1** exhibited a single rather broad absorption for the benzylic hydrogens of the dithiocarbamate ligands and similarly undifferentiated absorptions for the phenyl groups. This led us to speculate that the complexes were undergoing a previously unreported fluxional process and hence led us to a ^{13}C NMR study of the solution structure of **1**. Carbon NMR was the spectroscopy of choice because of the simplicity anticipated for spectra in the low-temperature limit, but the limited solubility of **1** (even in moderately polar solvents such as CH_2Cl_2) and the low sensitivity of natural abundance ^{13}C NMR required the use of samples which had been enriched at the

Table II. Fractional Atomic Coordinates (×10^4) and Equivalent Isotropic Displacement Coefficients[a] (Å × 10^3) for $[Mo_2O_3\{S_2CN(CH_2Ph)_2\}_4]\cdot 2CH_2ClCH_2Cl$

	x	y	z	U(eq)
Mo	1432(1)	9874(1)	4596(1)	35(1)
S(1)	1620(1)	10948(1)	4022(1)	39(1)
S(2)	2244(2)	10655(1)	6079(1)	42(1)
S(3)	1805(1)	9017(1)	5743(1)	44(1)
S(4)	3564(1)	9610(1)	4831(1)	41(1)
O(1)	0	10000	5000	48(2)
O(2)	1092(4)	9619(2)	3439(3)	56(2)
N(1)	2377(4)	11791(2)	5390(4)	39(2)
N(2)	4109(4)	8819(2)	6318(4)	38(2)
C(1)	2119(5)	11207(3)	5209(4)	34(2)
C(2)	2221(6)	12269(3)	4616(5)	45(2)
C(3)	2841(6)	12012(3)	6385(5)	49(2)
C(4)	3284(5)	9102(3)	5699(5)	36(2)
C(5)	3843(6)	8400(3)	7072(5)	45(2)
C(6)	5374(5)	8950(3)	6355(5)	40(2)
C(11)	1260(8)	13278(3)	4936(6)	63(3)
C(12)	282(10)	13624(4)	4950(7)	81(4)
C(13)	−793(10)	13392(5)	4650(8)	89(4)
C(14)	−925(8)	12776(5)	4375(7)	84(4)
C(15)	57(7)	12423(4)	4381(6)	60(3)
C(16)	1160(6)	12662(3)	4629(5)	47(2)
C(21)	4511(6)	12750(3)	6715(6)	59(3)
C(22)	5695(7)	12883(4)	6843(7)	71(3)
C(23)	6486(7)	12427(4)	6816(6)	69(3)
C(24)	6132(8)	11837(4)	6625(7)	71(3)
C(25)	4953(7)	11713(3)	6472(6)	63(3)
C(26)	4121(6)	12160(3)	6519(5)	47(2)
C(31)	4322(8)	7480(4)	6110(6)	65(3)
C(32)	4781(10)	6910(4)	6062(7)	84(4)
C(33)	5290(9)	6605(4)	6899(9)	85(4)
C(34)	5336(8)	6886(4)	7772(8)	77(4)
C(35)	4893(6)	7468(3)	7830(6)	54(3)
C(36)	4373(5)	7769(3)	7006(5)	43(2)
C(41)	5433(8)	9933(4)	7313(6)	61(3)
C(42)	5898(9)	10291(5)	8099(6)	82(4)
C(43)	6771(10)	10064(6)	8778(7)	90(4)
C(44)	7210(8)	9493(6)	8718(6)	88(4)
C(45)	6738(6)	9117(4)	7933(6)	63(3)
C(46)	5856(5)	9343(3)	7222(5)	43(2)
Cl(1)	9390(2)	10723(1)	10533(2)	92(1)
Cl(2)	7238(3)	10183(2)	11608(2)	135(2)
C(51)	9501(11)	10245(7)	11565(11)	154(7)
C(52)	8690(12)	9954(9)	11793(11)	197(10)

[a] Equivalent isotropic U defined as one-third of the trace of the orthogonalized U_{ij} tensor.

Table III. Selected Bond Lengths (Å) within $[Mo_2O_3\{S_2CN(CH_2Ph)_2\}_4]$ (**1**)

Mo–S(1)	2.495(3)	Mo–S(2)	2.710(3)
Mo–S(3)	2.444(3)	Mo–S(4)	2.506(3)
Mo–O(1)	1.863(2)	Mo–O(2)	1.677(5)
S(1)–C(1)	1.740(6)	S(2)–C(1)	1.692(6)
S(3)–C(4)	1.738(6)	S(4)–C(4)	1.706(7)
N(1)–C(2)	1.483(8)	N(1)–C(1)	1.323(8)
N(2)–C(4)	1.323(7)	N(1)–C(3)	1.471(8)
N(2)–C(6)	1.487(8)	N(2)–C(5)	1.460(9)

(20) Barral, R.; Bocard, C.; Sérée de Roch, I.; Sajus, L.; *Tetrahedron Lett.* **1972**, 1693.
(21) Matsuda, T.; Tanaka, K.; Tanaka, T. *Inorg. Chem.* **1979**, *18*, 454.

Table IV. Selected Bond Angles (deg) within $[Mo_2O_3\{S_2CN(CH_2Ph)_2\}_4]$ (**1**)

S(1)–Mo–S(2)	67.2(1)	S(1)–Mo–S(3)	155.5(1)
S(2)–Mo–S(3)	89.3(1)	S(1)–Mo–S(4)	96.8(1)
S(2)–Mo–S(4)	80.7(1)	S(3)–Mo–S(4)	71.3(1)
S(1)–Mo–O(1)	95.1(1)	S(2)–Mo–O(1)	83.8(1)
S(3)–Mo–O(1)	89.1(1)	S(4)–Mo–O(1)	155.0(1)
S(1)–Mo–O(2)	91.6(2)	S(2)–Mo–O(2)	157.9(2)
S(3)–Mo–O(2)	110.7(2)	S(4)–Mo–O(2)	96.5(2)
O(1)–Mo–O(2)	105.1(2)	Mo–S(1)–C(1)	92.2(2)
Mo–S(2)–C(1)	86.1(2)	Mo–S(3)–C(4)	87.7(2)
Mo–S(4)–C(4)	86.4(2)	Mo–O(1)–MoA	180
C(1)–N(1)–C(2)	122.9(5)	C(1)–N(1)–C(3)	121.8(5)
C(2)–N(1)–C(3)	115.3(5)	C(4)–N(2)–C(5)	122.5(5)
C(4)–N(2)–C(6)	122.2(5)	C(5)–N(2)–C(6)	115.1(5)
S(1)–C(1)–S(2)	114.5(3)	S(1)–C(1)–N(1)	121.4(5)
S(2)–C(1)–N(1)	124.1(5)	S(3)–C(4)–S(4)	113.8(3)
S(3)–C(4)–N(2)	122.4(5)	S(4)–C(4)–N(2)	123.7(5)

Table V. Fractional Atomic Coordinates ($\times 10^4$) and Equivalent Isotropic Displacement Coefficients[a] for $[Mo_2O_3(S_2CO^iPr)_4]$ (**5**)

	x	*y*	*z*	*U*(eq)
Mo	4250(1)	1060(1)	7311(1)	30(1)
S(1)	4226(1)	2051(2)	5794(1)	41(1)
S(2)	3338(1)	2159(3)	6731(1)	47(1)
S(3)	4200(1)	1083(2)	8959(1)	41(1)
S(4)	4439(1)	3622(2)	8077(1)	36(1)
O(1)	5000	917(8)	7500	37(2)
O(2)	4031(3)	−594(6)	7179(4)	47(2)
O(3)	3275(2)	3255(7)	5125(4)	45(2)
O(4)	4420(2)	3527(5)	9796(3)	38(2)
C(1)	3156(4)	4885(11)	3908(7)	57(3)
C(2)	3478(3)	3608(9)	4285(6)	46(3)
C(3)	3392(5)	2380(11)	3651(7)	73(4)
C(4)	4219(4)	3901(9)	11252(6)	52(3)
C(5)	4407(3)	2835(8)	10676(4)	35(2)
C(6)	4973(4)	2334(11)	11064(6)	57(3)
C(7)	3578(3)	2550(8)	5789(5)	39(2)
C(8)	4359(3)	2812(7)	9029(4)	30(2)

[a] Equivalent isotropic *U* defined as one-third of the trace of the orthogonalized U_{ij} tensor.

Table VI. Selected Bond Lengths (Å) within $[Mo_2O_3(S_2CO^iPr)_4]$ (**5**)

Mo–S(1)	2.455(2)	Mo–S(2)	2.540(2)
Mo–S(3)	2.501(2)	Mo–S(4)	2.728(2)
Mo–O(1)	1.878(1)	Mo–O(2)	1.691(6)
S(1)–C(7)	1.719(8)	S(2)–C(7)	1.695(8)
S(3)–C(8)	1.716(7)	S(4)–C(8)	1.677(7)
O(3)–C(7)	1.316(9)	O(3)–C(2)	1.495(11)
O(4)–C(8)	1.322(8)	O(4)–C(5)	1.486(8)

Table VII. Selected Bond Angles (deg) within $[Mo_2O_3(S_2CO^iPr)_4]$ (**5**)

S(1)–Mo–S(2)	71.0(1)	S(1)–Mo–S(3)	156.2(1)
S(2)–Mo–S(3)	95.9(1)	S(1)–Mo–S(4)	90.3(1)
S(2)–Mo–S(4)	80.5(1)	S(3)–Mo–S(4)	67.5(1)
S(1)–Mo–O(1)	89.9(1)	S(2)–Mo–O(1)	156.0(2)
S(3)–Mo–O(1)	96.3(1)	S(4)–Mo–O(1)	85.3(2)
S(1)–Mo–O(2)	108.4(2)	S(2)–Mo–O(2)	95.6(2)
S(3)–Mo–O(2)	92.3(2)	S(4)–Mo–O(2)	158.6(2)
O(1)–Mo–O(2)	104.4(3)	Mo–S(1)–C(7)	87.3(3)
Mo–S(2)–C(7)	85.1(3)	Mo–S(3)–C(8)	90.5(2)
Mo–S(4)–C(8)	83.9(2)	Mo–O(1)–MoA	171.6(5)
C(2)–O(3)–C(7)	120.2(6)	C(5)–O(4)–C(8)	121.1(5)
S(1)–C(7)–S(2)	116.5(4)	S(1)–C(7)–O(3)	124.1(6)
S(2)–C(7)–O(3)	119.3(6)	S(3)–C(8)–S(4)	118.1(4)
S(3)–C(8)–O(4)	123.0(5)	S(4)–C(8)–O(4)	118.9(5)

dithiocarboxy positions by preparation of the ligand from 99.9 atom % $^{13}CS_2$.

Variable-Temperature ^{13}C NMR Spectra of $[Mo_2O_3\{S_2{}^{13}CN(CH_2Ph)_2\}_4]$ and Evidence for Bridge/Terminal Oxo Exchange and Syn/Anti Isomerization. Room-temperature ^{13}C NMR spectra of **1** exhibit a single, broad absorption at δ 203.8 assignable to the enriched carbons of the dithiocarbamate ligands. As the

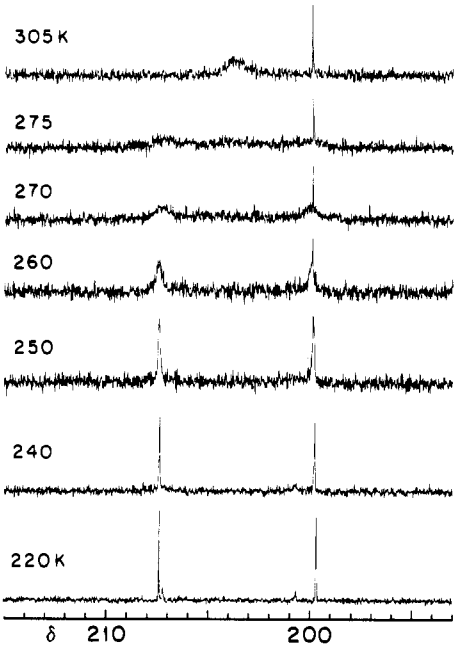

Figure 1. Variable-temperature ^{13}C NMR spectra of $[Mo_2O_3\{S_2{}^{13}CN(CH_2Ph)_2\}_4]$ from 220 to 305 K in CD_2Cl_2.

Scheme I

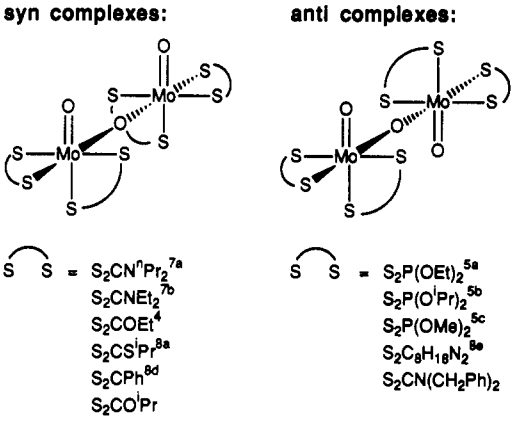

temperature is lowered (Figure 1), the broad singlet collapses and two new resonances of equal intensity appear at δ 207.4 and 199.8 at 250 K. As the temperature is lowered further, these signals separate again into two pairs of resonances which this time are of unequal intensity with the stronger signals at δ 207.4 and 199.7 and the weaker signals at δ 207.2 and 200.7 respectively at 220 K. The magnitude of this secondary splitting is slight. All of the temperature-dependent behavior is fully reversible upon warming.

The initial splitting of the room-temperature singlet into two equal intensity resonances suggested that the molecule is stereochemically nonrigid and undergoes an inter- or intramolecular dynamic process which equilibrates the dithiocarbamate ligands which have sulfur trans to the bridging oxo with the dithiocarbamate ligands with sulfur trans to the terminal oxo. Assignment of the quaternary signals at δ 207.4 and 199.8 to the dithiocarbamate ligands with a sulfur trans to the bridging oxo and to the dithiocarbamate ligands with a sulfur trans to the terminal oxo respectively is based on comparison with the quaternary ^{13}C NMR resonances for the Mo(IV) and Mo(VI) complexes $[MoO\{S_2CN(CH_2Ph)_2\}_2]$ (**2**) and $[MoO_2\{S_2CN(CH_2Ph)_2\}_2]$ (**3**) at δ 223.5 and 201.8—the average room temperature resonance for the Mo(V) complex **1** at δ 203.8 is in between these resonances, and it seems probable that the dithiocarbamate with a sulfur trans to the terminal oxo group is in the chemical environment which

Scheme II

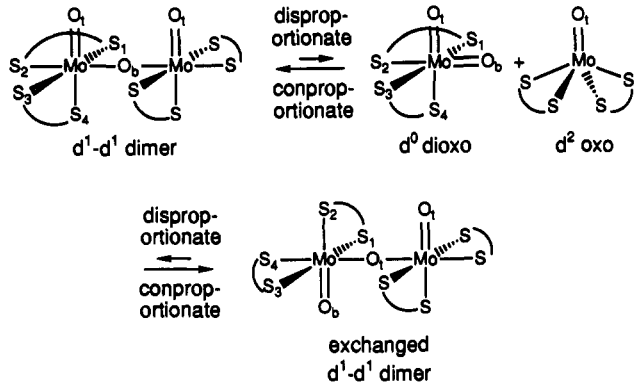

Scheme III

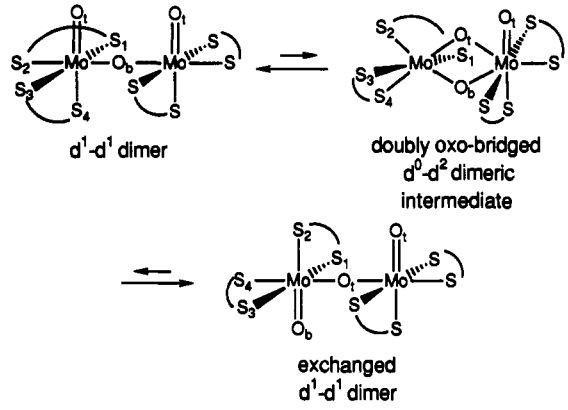

most closely resembles that in the Mo(VI) complex and hence has the higher field resonance.

The secondary splitting of the dithiocarbamate ligands into unequally populated groups was initially puzzling, but simple theory,[4] as mentioned above, does not anticipate energy difference between the syn and anti conformations of the $[Mo^{V}_2O_3]^{4+}$ core, and a reasonable interpretation is that **1** exists in solution as a mixture of the syn and anti isomers and that these are equilibriated above the coalescence point by the same dynamic process responsible for exchange of the dithiocarbamate ligands or by a second dynamic process (see below).

Possible Inter- and Intramolecular Bridge/Terminal Oxo Bridge Mechanisms within $[Mo_2O_3\{S_2{}^{13}CN(CH_2Ph)_2\}_4]$. The two most obvious candidates for the primary exchange process are shown in Schemes II and III. The first is an intermolecular process which involves the known ability of $[Mo^{V}_2O_3]^{4+}$ complexes to participate in thermal disproportionation equilibria which give $[Mo^{VI}O_2]^{2+}$ and $[M^{IV}O]^{2+}$ complexes,[20-22] and the second is an intramolecular pathway in which the dimer bends until one terminal oxo group coordinates to the other Mo center to give a dinuclear intermediate or transition state containing a six-coordinate Mo(IV) center and a seven-coordinate Mo(VI) center[23] connected by two bridging oxo atoms. This intermediate places both ligands at the six-coordinate Mo(IV) center trans to a bridging oxo atom. If the process is now reversed (with dissociation of the oxo atom that had originally been bridging), bridge and terminal oxo groups on one Mo atom will have exchanged and the corresponding dithiocarbamate ligands will also have exchanged.

The dimeric species in Scheme III could be a discrete intermediate but need only be an accessible transition state. As such, the existence of an isolable analog is not required for this species to be a resonable suggestion as part of a low-energy pathway for ligand interchange, but structural precedents would argue in favor of its energetic accessibility.

The simplest argument in favor of the plausibility of the doubly bridged dimer in Scheme III is that there are many Mo(V) oxo dimers with two bridging oxo groups instead of one. In fact, Mo(V) oxo dimers with four oxo groups rather than three (i.e. $[Mo_2O_4]^{2+}$ rather than $[Mo_2O_3]^{4+}$ cores) characteristically have two bridging oxo atoms as established crystallographically for a number of examples.[8g,25] These dimers typically have metal–metal interactions which spin-pair the d^1 metal centers, and a dative interaction between the d^2 center and the d^0 center would allow the proposed dimer to be electronically similar to the $[Mo_2O_4]^{2+}$ dimers.

It would also be reasonable to treat the dimer in Scheme III as containing discrete seven-coordinate Mo(VI) and six-coordinate Mo(IV) centers, and there is precedent in molybdenum chemistry for each of these geometry/oxidation state calibrations. The pentagonal bipyramidal Mo(VI) center is particularly well established, since Weiss's group showed some time ago that dithiocarbamato complexes of the $[MoOX_2]^{2+}$ (X = F, Cl, Br) core adopt pentagonal bipyramidal geometries.[26] This provides an interesting contrast with the usual preference for octahedral geometries exhibited by better known Mo(VI) cores such as the $[MoO_2]^{2+}$ unit (a change in preference which presumably reflects the replacement of a divalent oxo ligand with two univalent halides), and crystallographically characterized pentagonal bipyramid species like $[MoOCl_2(S_2CNEt_2)_2]$ provide excellent models for the Mo(VI) side of the dimer in Scheme III.

The more inocuous looking octahedral Mo(IV) side of the dimer is in fact more problematic, since in mononuclear systems octahedral $[MoX_2]^{2+}$-based complexes tend to prefer trans geometries as exemplified by $[Mo(acac)_2Cl_2]$ and related molecules.[27] There is, however, at least one crystallographically characterized case, that of $[Mo_2Cl_{10}]^{2-}$,[28] in which the geometric restrictions imposed by the need to use two ligands as bridges between two metal centers enforce a cis geometry analogous to that proposed for the Mo(IV) center in the dimer.

Distinguishing between Intermolecular and Intramolecular Exchange Mechanisms within $[Mo_2O_3\{S_2{}^{13}CN(CH_2Ph)_2\}_4]$. Although the key dissociative step in Scheme II is well precedented, it seemed unlikely that a dissociative process could provide a kinetically competent pathway for the dynamic process. The dissociation constants for the closely related Mo(V) dimers $[Mo_2O_3(S_2CNPr_2)_4]$[20] and $[Mo_2O_3(S_2CNEt_2)_4]$[21] have been established to be 4×10^{-3} mol L^{-1} in chlorobenzene and 2.0×10^{-3} mol L^{-1} in 1,2-dichloroethane respectively. It therefore seemed unlikely that there would be a sufficient concentration of the disproportionation products **2** and **3** to allow rapid

(22) Tanaka, T.; Tanaka, K.; Matsuda, T.; Hashi, K. In Ref 1d, p 361.
(23) The seven-coordinate Mo in Scheme III is drawn with a pentagonal bipyramidal geometry for convenience—capped octahedral or capped trigonal prismatic geometries are just as plausible, but we have no data on which to prefer any of the common seven coordinate geometries.[24] The actual geometry of this Mo in the transition state is relatively unimportant since the mechanism in Scheme III places no stereodynamic restrictions on this geometry.
(24) Kepert, D. L. *Prog. Inorg. Chem.* **1979**, *25*, 41.
(25) (a) Knox, J. R.; Prout, C. K. *Acta Crystallogr., B* **1969**, *25*, 1857. (b) Delbaere, L. T. J.; Prout, C. K. *J. Chem. Soc., Chem. Commun.* **1971**, 162. (c) Drew, M. G. B.; Kay, A. *J. Chem. Soc. A* 1971, 1846. (d) Ricard, L.; Martin, C.; Wiest, R.; Weiss, R. *Inorg. Chem.* **1975**, *14*, 2300. (e) Dance, I. G.; Wedd, A. G.; Boyd, I. W. *Aust. J. Chem.* **1978**, *31*, 519. (f) Cotton, F. A.; Morehouse, S. M. *Inorg. Chem.* **1965**, *4*, 1377. (g) Moynihan, K. J.; Boorman, P. M.; Ball, J. M.; Patel, V. O.; Kerr, K. A. *Acta Crystallogr., B* **1982**, *38*, 2258. (h) Cotton, F. A.; Ilsley, W. H. *Inorg. Chim. Acta* **1982**, *59*, 213. (i) Wieghardt, K.; Hahn, M.; Swiridoff, W.; Weiss, J. *Angew. Chem., Int. Ed. Engl.* **1983**, *22*, 491. (j) Beck, J.; Hiller, W.; Schweda, E.; Strähle, J. *Z. Naturforsch., B* **1984**, *39*, 1110.
(26) (a) Dirand, J.; Ricard, L.; Weiss, R. *Inorg. Nucl. Chem. Lett.* **1975**, *11*, 661. (b) Dirand, J.; Ricard, L.; Weiss, R. *J. Chem. Soc., Dalton Trans.* **1976**, 278.
(27) (a) van den Bergen, A.; Murray, K. S.; West, B. O. *Aust. J. Chem.* **1972**, *25*, 705. (b) Davies, J. E.; Gatehouse, B. M. *J. Chem. Soc., Dalton Trans.* **1974**, 184. (c) Kan, C.-T. *J. Chem. Soc., Dalton Trans.* **1982**, 2309.
(28) Hey, E.; Weller, F.; Dehnicke, K. *Z. Anorg. Allg. Chem.* **1984**, *508*, 86.

Table VIII. Barriers to Exchange of Dibenzyldithiocarbamate Ligands Trans to Bridging and Terminal Oxo Atoms in $[Mo_2O_3\{S_2{}^{13}CN(CH_2Ph)_2\}_4]$ (**1**) in 1,2-Dichloroethane at Various Temperatures: (a) As Determined from $w_{1/2}$ for the Quaternary Carbon Resonance Below Coalescence; (b) As Determined from $\Delta\nu$ at Coalescence; (c) As Determined from $w_{1/2}$ of the Averaged Quaternary Carbon Resonance and $\Delta\nu$ above Coalescence[a]

T, K	$w_{1/2}$, Hz	k, Hz	$\Delta G^{\ddagger}$, kcal mol^{-1}
		Part a	
240 ± 0.5	4.0 ± 1		
245 ± 0.5	8.0 ± 2	12.6 ± 3	13.0 ± 0.2
250 ± 0.5	9.8 ± 2	18.2 ± 3	13.1 ± 0.2
255 ± 0.5	10.6 ± 2	20.7 ± 3	13.3 ± 0.2
		Part b	
290 ± 0.5		2 080 ± 25	12.6 ± 0.3
		Part c	
320 ± 0.5	90 ± 9	16 000 ± 1 600	12.6 ± 0.7
325 ± 0.5	55 ± 7	27 100 ± 3 400	12.5 ± 0.1
330 ± 0.5	46 ± 5	32 900 ± 3 600	12.6 ± 0.9
335 ± 0.5	37 ± 2	41 900 ± 5 700	12.6 ± 0.7

[a] $\Delta\nu$ = 938 Hz.

dissociative isomerization of **1**—we do see some **3** in ^{13}C NMR spectra of labeled **1** (e.g. at δ 199.8 in Figure 1), but this **3** is a byproduct of decomposition of **1** in halocarbon NMR solvents, as established by its slow increase over time. We see no **2** as would be anticipated if the disproportionation equilibrium were readily accessible thermally.

Direct experimental support for an intramolecular isomerization pathway within **1**, such as that in Scheme III, comes from the value of the exchange barrier as determined from the line width of the resonance of the averaged quaternary carbons above coalescence and the quaternary carbons trans to the terminal or bridging oxo groups below coalescence. Data suitable for quantitative analysis were obtained in CH_2ClCH_2Cl and are summarized in Table VIII, together with the derived exchange rates and $\Delta G^{\ddagger}$ obtained as described in the Experimental Section (line widths determined in CD_2Cl_2 gave values for $\Delta G^{\ddagger}$ indistinguishable from those in CH_2ClCH_2Cl but were only available over a restricted range of temperatures in this low boiling solvent). The small magnitude (12.6 kcal mol^{-1} above coalescence) of $\Delta G^{\ddagger}$ for the exchange constitutes an immediate argument against the intermolecular mechanism in Scheme II—Matsuda et al.[21,22] have previously reported a value of 17.0 ± 2.1 kcal mol^{-1} for $\Delta G^{\ddagger}$ for disproportionation of the closely related complex $[Mo_2O_3(S_2CNEt_2)_4]$ in 1,2-dichloroethane at 25 °C, and the comparison between this value and the data in Table VIII confirms our opinion that disproportionation does not provide a kinetically competent initial step for the exchange process in **1**.

The agreement between the activation barriers in Table VIII determined from line widths above and below coalescence is acceptable but not outstanding, and this probably reflects systematic errors in values determined using the slow exchange approximation. These arise because of the influence on linewidths of the incipient splitting of the δ 207.4 and 199.8 peaks into components arising from the syn and anti isomers. We therefore prefer the values determined in the fast exchange approximation.

The availability of $\Delta G^{\ddagger}$ values at several temperatures within the range covered by the fast exchange approximation in 1,2-dichloroethane allowed separation of $\Delta G^{\ddagger}$ into its enthalpic and entropic components (Table IX) and hence provided further support for an intramolecular exchange mechanism. As is obvious from the insensitivity of $\Delta G^{\ddagger}$ to variations in temperature, $\Delta S^{\ddagger}$ is negligible—this argues strongly against an intermolecular mechanism for the exchange process.

Relationship Between Syn/Anti Isomerization and Bridge/Terminal Oxo Exchange within $[Mo_2O_3\{S_2{}^{13}CN(CH_2Ph)_2\}_4]$. The intramolecular bridge/terminal oxo exchange reaction in Scheme III allows simultaneous syn/anti isomerization, a reaction which must be rapid on the NMR time scale if we are to average the signals from these isomers as the temperature of the sample is raised above that at which the low-temperature limiting spectrum is observed.

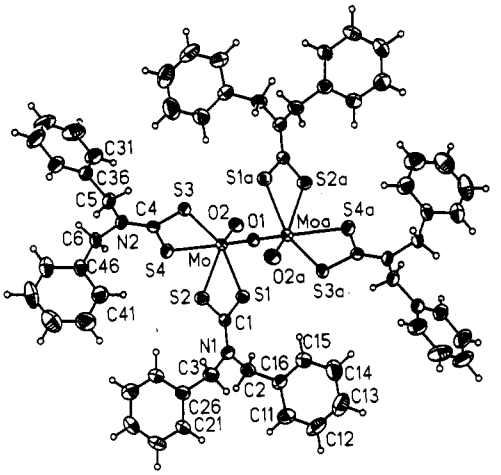

Figure 2. Molecular structure of $[Mo_2O_3\{S_2CN(CH_2Ph)_2\}_4]$ (40% probability ellipsoids). Atoms with an "a" subscript are symmetry generated by inversion through the bridging oxygen.

Table IX. Activation Parameters for the Exchange of Bridging and Terminal Oxo Atoms in $[Mo_2O_3L_4]$ Complexes As Determined by Plots of $\Delta G^{\ddagger}$ versus Temperature for Data Obtained from Line Width Data above Coalescence

L	$\Delta G^{\ddagger}_{295}$, kcal/mol^{-1}	$\Delta H^{\ddagger}$, kcal mol^{-1}	$\Delta S^{\ddagger}$, cal K^{-1} mol^{-1}
$S_2CN(CH_2Ph)_2$	+12.6 ± 0.1	+11.9 ± 0.4	−2.0 ± 0.6
S_2COEt	+12.3 ± 0.1	+11.1 ± 0.3	−3.9 ± 1.2
S_2CO^iPr	+12.3 ± 0.1	+12.9 ± 0.4	+1.9 ± 0.6

The proposal that the observed syn/anti isomerization is a byproduct of bridge/terminal oxo exchange was attractive because of its simplicity, but it seemed plausible initially that syn/anti isomerization could involve a second dynamic process such as counterrotation of the two Mo coordination spheres about the Mo–O–Mo axis. We have, however, determined (as described in the Experimental Section) that the secondary exchange barrier is 15.8 ± 3 kcal mol^{-1}, a value close to that determined for the primary exchange process. The equality of these primary and secondary barriers establishes that it is unnecessary to hypothesize syn/anti isomerization mechanisms beyond that shown in Scheme III, although it remains possible (if unlikely) that rotation is a kinetically accessible syn/anti isomerization mechanism under these conditions and happens to have activation parameters similar to those for bridge/terminal oxo exchange.

Ground-State Isomers of $[Mo_2O_3\{S_2CN(CH_2Ph)_2\}_4]$ in the Solid State and in Solution. The observation of facile interconversion of syn and anti isomers of **1** in solution led us to determine the molecular structure of **1** in the solid state by means of the single-crystal X-ray diffraction study described in the Experimental Section. This enabled us to determine that **1** has the molecular structure shown in Figure 2 and that the crystal contains a molecule of 1,2-dichloroethane of solvation per dimer unit. Complex **1** resides on a crystallographic inversion center at (0, 1, $^1/_2$). This requires that the Mo(1)–O(1)–Mo(2) angle be exactly 180°. Each Mo atom has a distorted octahedral coordination geometry with cis angles ranging from 67.2(1) to 110.7(2)° and trans angles ranging from 155.0(1) to 157.9(2)°. The terminal Mo=O$_t$ bond length of 1.677(5) Å agrees well with other Mo=O$_t$ bond lengths in the literature, and the Mo–O$_b$ bond length of 1.863(2) Å is within the range reported for analogous distances in other $[Mo^{V}_2O_3]^{4+}$ complexes.[3-8] The Mo—S(2) bond, trans to M=O$_t$(2), is 2.710(3) Å, while the remaining Mo—S bonds range from 2.444(3) to 2.506(3) Å.

The most interesting feature of the molecular structure of **1** is the anti orientation adopted by the Mo=O$_t$ groups. This is

analogous to the anti orientation which we have previously established for the $[W_2O_3]^{4+}$ groups in $[W_2O_3\{S_2CN(CH_2Ph)_2\}_4]$,[9] isologous with **1**, and to the anti orientations established for dithiophosphate and thiocyanate dimers,[5,6] but is in sharp contrast with the syn orientation adopted by other structurally characterized dithiocarbamate complexes of the $[Mo^{V}_2O_3]^{4+}$ unit.[7]

This is an intriguing observation, and the fact that the preference for an anti conformation is independent of the metal in **1** and its W isolog but that dithiocarbamate complexes of $[Mo_2O_3]^{4+}$ units with other R groups adopt a syn conformation[7] is consistent with the earlier suggestion[4] that syn/anti preferences in $[M_2O_3]^{4+}$ complexes are not controlled by electronic factors. The solid-state preferences must arise from combinations of secondary effects such as intramolecular steric interactions and solid-state packing forces, and the syn/anti mixture observed in solutions of **1** at −28 °C establishes that the free energy differences between the isomers in solution at this temperature is only 0.6 kcal mol^{-1}. This small ΔG makes it meaningless to infer the identity of the major isomer in solution on the basis of the solid-state structure.

Variable-Temperature ^{13}C NMR Spectra of the Xanthate Complexes $[Mo_2O_3(S_2{}^{13}COEt)_4]$ and $[Mo_2O_3(S_2{}^{13}CO^{i}Pr)_4]$. The evidence in favor of an intramolecular mechanism for bridge/terminal oxo exchange within **1** raised the question of whether such exchange reactions are a general characteristic of the $[Mo^{V}_2O_3]^{4+}$ unit within other ligand environments and hence suggested carbon NMR studies of other $[Mo_2O_3]^{4+}$ complexes.

Xanthate complexes are attractive candidates for such studies since the dithiocarboxylate ligands can be prepared with ^{13}C labels by a simple addition of alkoxides to $^{13}CS_2$.[12,15] More significantly, xanthate ligands are sufficiently similar to dithiocarbamates that we could anticipate bridge/terminal oxo exchange reactions similar to those observed for **1** if the reaction is intramolecular, but Mo(VI) monomers of the type $[Mo^{VI}O_2(S_2COR)_4]$ are believed to be unstable (largely because of the failure of attempts to prepare them),[12,15] and xanthate complexes of $[Mo^{V}_2O_3]^{4+}$ cores are therefore less likely to participate in disproportionation equilibria which would allow access to intermolecular bridge/terminal exchange mechanisms such as that shown in Scheme II.

The particular xanthate dimers chosen for study were the ethyl complex $[Mo_2O_3(S_2{}^{13}COEt)_4]$ (**4**), one of the most extensively studied xanthate complexes,[4,15] and the isopropyl complex $[Mo_2O_3(S_2{}^{13}CO^{i}Pr)_4]$ (**5**),[12] chosen because the increased bulk of the ligand might shed some light on the importance of intramolecular steric bulk in these systems.

The quaternary carbon of the ethyl xanthate complex **4** gives rise to a ^{13}C signal in $CDCl_3$ at δ 227.1 at 300 K. This signal sharpens upon warming, and splits into singlets of equal intensity at δ 231.2 and 220.7 as the temperature is lowered to 260 K (Figure 3). These signals split further into high intensity singlets at δ 231.3 and 220.3 and weaker singlets at δ 230.9 and 222.0 as the temperature is lowered further to 230 K. Similarly, the quaternary carbon of the isopropyl xanthate complex **5** gives a ^{13}C signal in $CDCl_3$ at δ 225.7 at 290 K. This signal again sharpens upon warming and splits into singlets of equal intensity at δ 229.8 and 220.3 as the temperature is lowered (Figure 4), in this case to 250 K. The upfield signal is split further at lower temperatures into a large singlet at δ 219.4 and a small singlet at δ 221.0. The downfield singlet does not split further, but a shoulder appears on its upfield side.

The temperature-dependent ^{13}C NMR spectra of **4** and **5** indicate that both xanthate complexes are fluxional and that xanthate ligands trans to bridging oxo groups exchange rapidly on the NMR trans scale with xanthate groups trans to terminal oxo groups. Since Mo(VI) xanthate oxo compounds are unknown we do not have a reference set of Mo(VI) ^{13}C data with which to make comparisons, but we again assign the higher field resonances to ligands trans to terminal oxo groups by analogy with the dithiocarbamate data above.

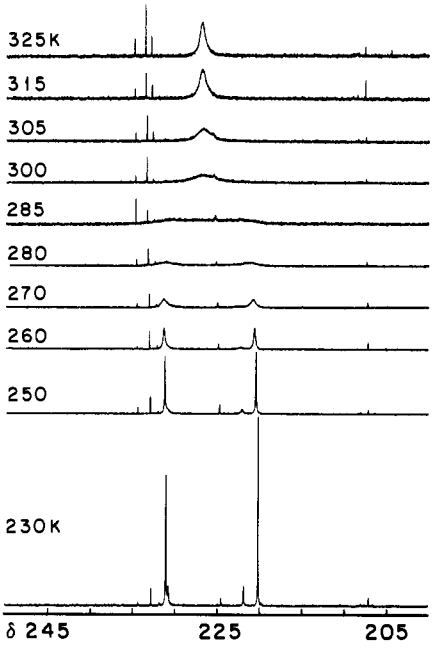

Figure 3. Variable-temperature ^{13}C NMR spectra of $[Mo_2O_3(S_2{}^{13}COEt)_4]$ from 230 to 325 K in $CDCl_3$.

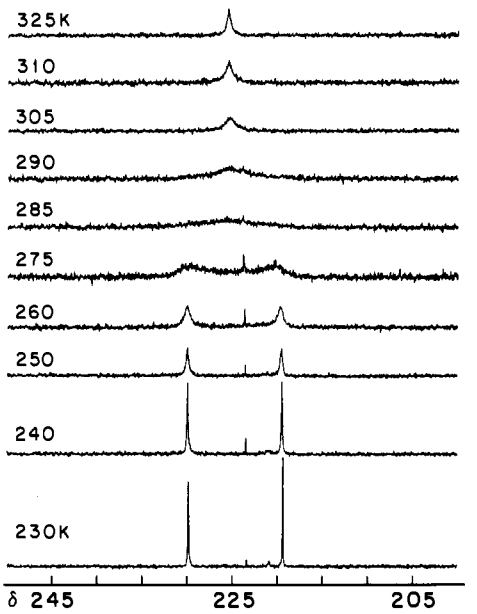

Figure 4. Variable-temperature ^{13}C NMR spectra of $[Mo_2O_3(S_2{}^{13}CO^{i}Pr)_4]$ from 230 to 325 K in $CDCl_3$.

The secondary splittings of the xanthate resonances into set peaks of unequal intensity again suggest that the complexes exist as an equilibrium mixture of syn and anti isomers in solution.

Ground-State Isomers of $[Mo_2O_3(S_2O^{i}Pr)_4]$ in the Solid State and in Solution. It has been previously established that the ethyl xanthate complex **4** adopts a syn conformation in the solid state,[4] but the increased bulk of the isopropyl ligand in **5** raised the possibility that **5** might adopt an anti conformation in the solid state. We therefore carried out the single-crystal X-ray diffraction study described in the Experimental Section, and established that **5** adopts a similar syn conformation in the solid state (Figure 5). This indicates that the increase in the bulk of the alkyl substituent on going from the ethylxanthate complex **4** to the isopropyl xanthate complex **5** does not give rise to sufficient intramolecular steric intervention to disfavor the syn isomer in the solid state.

As in the case of **1** it is tempting to assume a relationship between the solid-state syn conformational preferences of **4** and **5** and their solution conformational preferences, but the observation of both conformers **4** and of **5** in solution establishes that

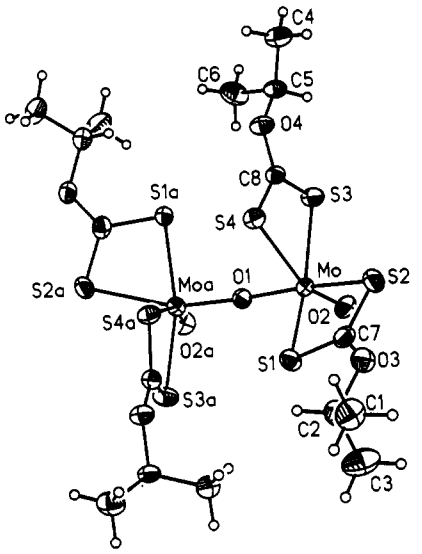

Figure 5. Molecular structure of $[Mo_2O_3(S_2CO^iPr)_4]$ (40% probability ellipsoids). Atoms with an "a" subscript are symmetry generated by rotation about the 2-fold axis.

there is only a small intrinsic free energy difference between the two conformers with both ligands (0.9 and 1.0 kcal mol^{-1} respectively for **4** and **5**) and hence that the solid-state preference could be controlled by minimal differences in packing energies rather than by an intramolecular electronic or steric factors.

Details of the solid-state structure of **5** are unexceptional. There is half a molecule in the asymmetric unit with a crystallographic 2-fold axis along $^1/_2$, y, $^3/_4$). There is an essentially linear oxo bridge of 171.6(5)° between the Mo centers, and a torsion angle of 8.3° between the terminal oxo atoms as viewed along the Mo–O–Mo axis. The Mo atoms have distorted octahedral coordination geometries with Mo–O_b bond lengths of 1.877(1) Å and Mo–O_t bond lengths of 1.684(6) Å. These parameters reflect the partial double bond character of the bridging oxo bonds and the full double bond character of the terminal oxo bonds. The Mo–S bond lengths vary, with the Mo-S(4) bond trans to the Mo=O_t bond much the longest at 2.728(2) Å while the remaining Mo-S bonds range from 2.455(2) to 2.540(2) Å. There is a disordered solvent molecule, believed to be toluene, which was not refined.

Kinetic Parameters for the Fluxional Processes within $[Mo_2O_3(S_2{}^{13}COEt)_4]$ and $[Mo_2O_3CO^iPr)_4]$. The resemblance between the variable-temperature ^{13}C NMR spectra of **4** and **5** and those of **1** is quantitative as well as qualitative. Exchange rates for the primary dynamic process equilibrating xanthate ligands with a suflur trans to a terminal oxo with xanthates with a sulfur trans to a bridging oxo were determined at a variety of temperatures both from linewidth measurements and from coalescence temperatures as described in the Experimental Section, and these rates and the derived free energy barriers to exchange are summarized in Tables X and XI for complexes **4** and **5** respectively. Inspection of these tables establishes that the ΔG^* are indistinguishable for **4** and **5**, and at *ca.* 12.3 kcal mol^{-1} above coalescence are essentially identical to the corresponding value of 12.6 kcal mol^{-1} for **1**. We have also used the values of ΔG^* determined from line-width measurements above coalescence (which we prefer for reasons discussed above in the case of **1**) to determine the enthalpic and entropic contributions to ΔG^* as summarized in Table IX.

The activation parameters for the dynamic processes occurring within **4** and **5** strongly suggest that these are intramolecular processes since there are only negligible entropic contributions to the activation barriers, and we propose that they involve a bridge/terminal oxo exchange mechanism analogous to that outlined for **1** in Scheme III. This would account for both the xanthate exchange reaction and for the syn/anti isomerization

Table X. Barrier to Exchange of Ethyl Xanthate Ligands Trans to Bridging and Terminal Oxo Atoms in $[Mo_2O_3(S_2{}^{13}COEt)_4]$ in $CDCl_3$ at Various Temperatures: (a) As Determined from $w_{1/2}$ for the Quarternary Carbon Resonance Below Coalescence; (b) As Determined from $\Delta\nu$ at Coalescence; (c) As Determined from $w_{1/2}$ of the Averaged Quaternary Carbon Resonance and $\Delta\nu$ above Coalescence[a]

T, K	$w_{1/2}$, Hz	k, Hz	ΔG^*, kcal mol^{-1}
		Part a	
230 ± 0.5	7.5 ± 2		
250 ± 0.5	13.8 ± 2	19.8 ± 3	13.1 ± 0.1
260 ± 0.5	33.8 ± 2	82.6 ± 3	12.9 ± 0.1
270 ± 0.5	93.8 ± 2	271 ± 3	12.8 ± 0.1
280 ± 0.5	263 ± 2	803 ± 3	12.7 ± 0.1
		Part b	
283 ± 0.5		3 020 ± 20	12.1 ± 0.1
		Part c	
290 ± 0.5	788 ± 2	3 720 ± 44	12.2 ± 0.1
300 ± 0.5	376 ± 2	7 880 ± 96	12.2 ± 0.1
305 ± 0.5	275 ± 2	10 900 ± 130	12.3 ± 0.1
310 ± 0.5	219 ± 2	13 700 ± 163	12.3 ± 0.1
315 ± 0.5	158 ± 2	19 300 ± 230	12.3 ± 0.1
320 ± 0.5	120 ± 2	25 800 ± 310	12.3 ± 0.1
325 ± 0.5	93.8 ± 2	33 700 ± 400	12.3 ± 0.1

[a] $\Delta\nu$ = 1360 ± 2 Hz.

Table XI. Barrier to Exchange of Isopropyl Xanthate Ligands Trans to Bridging and Terminal Oxo Atoms in $[Mo_2O_3(S_2{}^{13}CO^iPr)_4]$ in $CDCl_3$ at Various Temperatures: (a) As Determined from $w_{1/2}$ for the Quaternary Carbon Resonance below Coalescence; (b) As Determined from $\Delta\nu$ at Coalescence; (c) As Determined from $w_{1/2}$ of the Averaged Quaternary Carbon Resonance and $\Delta\nu$ above Coalescence[a]

T, K	$w_{1/2}$, Hz	k, Hz	ΔG^*, kcal mol^{-1}
		Part a	
225 ± 0.5	6.4 ± 2		
230 ± 0.5	8.6 ± 2		
240 ± 0.5	11.8 ± 2	17.0 ± 3	12.6 ± 0.1
250 ± 0.5	22.5 ± 2	50.6 ± 3	12.6 ± 0.1
260 ± 0.5	55.7 ± 2	155 ± 3	12.6 ± 0.1
270 ± 0.5	114 ± 2	338 ± 3	12.6 ± 0.1
		Part b	
284 ± 0.5		1 750 ± 20	12.4 ± 0.1
		Part c	
290 ± 0.5	257 ± 2	3 880 ± 48	12.2 ± 0.1
295 ± 0.5	209 ± 2	4 800 ± 73	12.3 ± 0.1
305 ± 0.5	88.9 ± 2	11 800 ± 430	12.2 ± 0.1
310 ± 0.5	55.7 ± 2	19 700 ± 600	12.1 ± 0.1
315 ± 0.5	53.6 ± 2	20 600 ± 1300	12.3 ± 0.1
325 ± 0.5	34.3 ± 2	34 900 ± 3700	12.3 ± 0.1

[a] $\Delta\nu$ = 787 ± 2 Hz.

Table XII. Free Energies of Activation for the Secondary Exchange Barriers in $[Mo_2O_3L_4]$ Complexes As Estimated by the Method of Shanan-Atidi and Bar-Eli[19]

L	T, K	dG^*_A, kcal mol^{-1}	ΔG^*_B, kcal mol^{-1}
$S_2CN(CH_2Ph)_2$	220 ± 0.2	15.8 ± 3.2	15.3 ± 3.1
S_2COEt	240 ± 0.2	12.7 ± 2.5	14.2 ± 2.8
S_2CO^iPr	240 ± 0.2	13.0 ± 2.6	14.5 ± 2.9

which appears as a secondary process. The precision of the data do not allow a highly precise independent determination of the syn/anti exchange barriers in **4** and **5**, but we have been able to determine approximate values of ΔG^* as described in the Experimental Section. The resulting free energies of activation (Table XII—this includes the data for **1** for comparison) are identical within experimental error to those determined for the primary exchange process, and the data do not require the hypothesis of a syn/anti isomerization mechanism beyond that provided by the intramolecular bridge/terminal oxo exchange reaction shown in Scheme III.

Conclusion

The dithiocarbamate and xanthate $[Mo^{V}_{2}O_{3}]^{4+}$ complexes **1**, **4**, and **5** are all fluxional on the NMR time scale, and participate in dynamic processes which equilibrate the bischelating ligands. For all three compounds the activation parameters associated with this dynamic process strongly suggest an intramolecular mechanism which we propose involves the bridge for terminal oxo exchange reaction shown in Scheme III. This would also result in interconversion of the syn and anti isomers of **1**, **4**, and **5**, a process which is indeed observed to be fast on the NMR time scale for all three complexes.

The most convincing argument in favor of an intramolecular bridge/terminal oxo exchange process to account for the fluxionality of **1**, **4**, and **5** is the marked similarity of the parameters determined for the dithiocarbamate complex **1** and for the xanthate complexes **4** and **5**. It is well established that the disproportionation equilibria of $[Mo^{V}_{2}O_{3}]^{4+}$ complexes are highly sensitive to the ancillary ligands, and the similarity of the parameters would be a remarkable coincidence if the exchange process is dissociative (Scheme II) rather than intramolecular as shown in Scheme III.

The similarity of the energetic parameters for exchange of **1**, **4**, and **5** also argues against alternative intramolecular exchange processes such as dissociation of one sulfur of a dithiocarboxylate ligand to give a species with a five-coordinate molybdenum center. Such an intermediate would almost certainly have a low barrier to rearrangement,[29] but partial decomplexation of a bischelating dithiocarboxylate ligand seems intrinsically unlikely and it is highly improbable that the barrier to such a process would be identical for dithiocarbamate and xanthate ligands.

Intramolecular bridge/terminal oxo exchange in $[Mo^{V}_{2}O_{3}]^{4+}$ complexes has not previously been suggested, and its existence, facility, and probable generality adds an interesting dimension to the chemistry of this class of molecules. These systems are of considerable interest in their own right, and although they do not participate directly in the Mo(VI)/Mo(IV) oxo transfer reactions central to the chemistry of molybdenum-based oxo transferases, understanding their chemistry is critical to our understanding of the biological systems because of the pervasive formation of $[Mo^{V}_{2}O_{3}]^{4+}$ complexes by conproportionation of $[Mo^{VI}O_{2}]^{2+}$ and $[Mo^{IV}O]^{2+}$ monomers, as has been recently emphasized.[2]

Acknowledgment. This work was supported in part by the Office of Naval Research.

Supplementary Material Available: Complete tables of bond lengths (Tables IS, IIS); bond angles (Tables IIIS, IVS), anisotropic displacement coefficients (Tables VS, VIS), hydrogen atom coordinates, and isotropic thermal parameters (Tables VIIS, VIIIS) (8 pages). Ordering information is given on any current masthead page.

(29) Kepert, D. L. In *Comprehensive Coordination Chemistry*; Wilkinson, G., Gillard, R. D., McCleverty, J. A., Eds.; Pergamon: Oxford, England, 1987; Vol. 1, Chapter 2.2.